Article

A Paper-Chip-Based Phage Biosensor Combined with a Smartphone Platform for the Quick and On-Site Analysis of *E. coli* O157:H7 in Foods

Chaiyong Wu [1], Dengfeng Li [2], Qianli Jiang [3] and Ning Gan [2,*]

[1]   School of Material Science and Chemical Engineering, Ningbo University, Ningbo 315211, China
[2]   School of Oceanography, Ningbo University, Ningbo 315211, China
[3]   Southern Hospital of Nanfang Medical University, Guangzhou 510515, China
[*]   Correspondence: ganning@nbu.edu.cn

Abstract: The rapid and specific point-of-care (POC) analysis of virulent pathogenic strains plays a key role in ensuring food quality and safety. In this work, a paper-based fluorescent phage biosensor was developed for the detection of the virulent *E. coli* O157:H7 strain (as the mode of virulent pathogens) in food samples. Firstly, phages that can specifically combine with *E. coli* O157:H7 (*E. coli*) were stained with SYTO-13 dye to prepare a novel fluorescent probe (phage@SYTO). Simultaneously, a micro-porous membrane filter with a pore size of 0.45 μm was employed as a paper chip so as to retain the *E. coli*-phage@SYTO complex (>1.2 μm) on its surface. The phage@SYTO (200 nm in size) was able to pass through the pores of the chip, and the complex could be retained on the paper chip using the free phage@SYTO probes. The *E. coli*-phage@SYTO could emit a visual fluorescent signal (excited at 365 nm; emitted at 520 nm) onto the chip, which could be detected by a smartphone to reflect the concentration of *E. coli*. Under optimized conditions, the detection limit was as low as 50 CFU/mL (S/N = 3) and exhibited a wide linear range from 10^2 to 10^6 CFU/mL. The sensor has potential application value for the quick and specific POCT detection of virulent *E. coli* in foods.

Keywords: POCT assay; paper-chip-based phage biosensor; smartphone; *E. coli* O157:H7; foods

1. Introduction

Threats to food safety caused by pathogenic bacteria infections have given rise to serious damage worldwide and resulted in serious losses in livestock husbandry, agriculture, and aquaculture [1–4]. To preserve food security, early diagnostic methods for foodborne pathogens should be developed so as to prevent pathogenic infections in advance [5–7]. Moreover, there is a great need to develop rapid on-site assays for the identification of pathogenic bacterial strains because the virulence of different strains of the same bacteria varies greatly; for example, *E. coli* O157:H7 is significantly more virulent than other *E. coli* strains.

The conventional culture-based bacterial detection assays are cumbersome and tedious [8,9]. Due to their high equipment and laboratory environment requirements, nucleic-acid-based polymerase chain reaction (PCR) detection methods can discriminate different strains of the same bacteria, but are not conducive to large-scale promotion, especially in resource-limited areas [10,11]. The fabrication of a commercial point-of-care (POC) diagnostic platform has become a cutting-edge and challenging task in the field of rapid on-site analysis [1]. It is hoped that such a platform will be able to perform quick, user-friendly analysis through a cheap, automatic, and easily operated setup. The paper-chip-based biosensor is a promising alternative for the detection of samples because of its visual and sensitivity properties [12,13]. As the base of the analytical platform, paper has the advantages of a low cost, liquid flow features, biodegradability, and good chemical properties, and it has been widely used in various analytical systems. Compared with traditional

analytical chips, the paper-chip-based analytical platform does not require external fluid pumping equipment or a complex chip design, and can be used for sample sampling and delivery through the capillaries of paper fibers. In addition, paper chips with different pore sizes can also be employed as filter membranes to be used for enriched or filter bacteria. As this method is suitable for mass production, it has attracted much attention.

In addition, the combination of paper chips and a smartphone can fulfill the requirements for fabricating field devices with good sensitivity and specificity [14–17]. Being easy to operate and carry, smartphones have attracted great attention in healthcare, environmental monitoring, and the on-site analysis of food production [18,19]. With the proliferation of smartphones, their digital imaging capabilities render them an excellent analytical platform for the development of instant detection sensors. Compared to single-emission fluorescence detection, the proportional fluorescence detection method used in this experiment has a built-in self-calibration function that avoids interference caused by various target-independent factors and circumvents/reduces the output of false-positive results, thereby improving the detection accuracy and extending the dynamic detection range for complex food matrices [20]. Aiming to recognize a specific bacterial strain, biological probes are essential for fabricating paper-chip-based sensors. Phages are viruses that attack and eat bacteria and are mainly composed of nucleic acids and protein shells [15,21]. The shell of the phage can specifically combine with the receptor on the surface of the host bacteria, and its genetic material, DNA, or RNA can be injected into the host bacteria. Compared with antibodies, phages exhibit much higher specificity towards bacterial strains [22–24]. Moreover, they have a higher affinity for live strains. Therefore, phage probes can be employed to establish paper chips for the POC detection of *E. coli* O157:H7. [15,16] Their signal changes marking the emergence of pathogenic bacteria can be monitored by the biosensors and detected by the smartphone [17,25–27].

Hence, herein, we propose a novel paper-based phage sensor using a phage probe integrated with a smartphone for the visual detection of *E. coli* O157:H7 based on RGB values. The fabrication of the phage probe and the sensor is shown in Figure 1. Firstly, the phage, which can specifically combine with *E. coli* O157:H7 (*E. coli*), was stained with SYTO 13 florescence dye, a universal DNA embedding dye [17,18], to prepare the phage@SYTO probe. The probes were mixed with samples containing the bacteria that would specifically combine with the target *E. coli* of the *E. coli*-phage@SYTO complex (>1.2 nm) and be retained on the paper chip (the filter membrane with a pore size of 0.45 μm). The free phage@SYTO probes, with a size of approximately 200 nm, can pass through the pores of the paper chip. Thus, the conjugate complex (*E. coli* phage@SYTO) can easily be separated from the free probes and enriched on the paper chips. In the next step, the complex was excited by 365 nm light using a green fluorescence light with an emission wavelength of 520 nm, which can be visually observed and recorded by a smartphone. The G value from RGB was employed for the quantification of the target bacteria. The sensor was also successfully employed to detect *E. coli* in food samples.
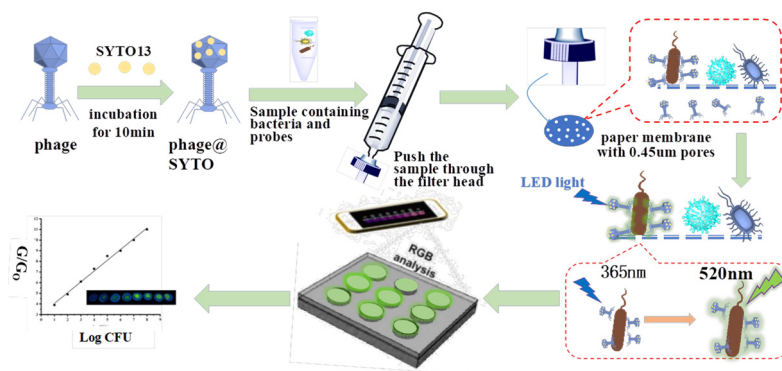

Figure 1. The preparation of the phage@SYTO probe and detection of *E. coli* O157:H7. based on a paper chip biosensor.

2. Materials and Methods

2.1. Chemicals

SYTO-13 (99.5% wt) was obtained from Macklin Co., Ltd. (Shanghai, China) (250 μL, 5 mmol). Phages of E. coli O157:H7 were screened at Dr Dengfeng Li's lab. The strains used in this study included *Vibrio parahaemolyticus* (*V. P*, ATCC 17802), *Salmonella typhimurium* (*S. T*, ATCC 14028), and *Staphylococcus aureus* (*S. A*, ATCC 43300), which were purchased from Shanghai Luwei Technology Co., Ltd. (Shanghai, China); *Listeria monocytogenes* (*L. M*, CICC 21662), which was purchased from the China Industrial Culture Collection (CICC); and *Escherichia coli* O157:H7 (ATCC 25922), obtained from Dengfeng Li's group at Ningbo University. Cellulose membrane filters with pore sizes of 0.10, 0.22, 0.45, 0.65, and 1.00 μm were purchased from Shanghai Luwei Technology Co., Ltd. (Shanghai, China). The LB broth and agar powder (bacterial grade) were derived from Hangzhou Microbial Reagent Co., Ltd. (Hangzhou, China).

2.2. Apparatus

The fluorescence, probe excitation, and emission spectra were measured using a fluorescence spectrophotometer which was purchased from Shimadzu Co., Ltd. (Kyoto, Japan). The centrifuge was purchased from Sigma Laborzentrifugen GmbH (Berlin, Germany). The medical constant temperature incubator was purchased from Panasonic Appliances Cold Chain Co., Ltd. (Tokyo, Japan). The desktop constant temperature oscillator was purchased from Jiemei Electronics Co., Ltd. (Suzhou, China). We used a transmission electron microscope (TEM, JEM 2100F, Tokyo, Japan). The FL images were captured via an Android smartphone (model number: Xiaomi 11X hypercharge, with camera specifications of 64 MP/26 mm wide). A 365 nm LED light was placed above the sample, positioned over one side. The distance from the excited LED light source to the sample remained constant (5 cm) during the measurement. Color analysis software was used to divide the color fluorescence image of the sample into red (R), green (G), and blue (B) pixels. In the required analysis, we added different concentrations of bacteria ($10 \sim 10^8$ CFU/mL) to the solution, each on a different piece of paper. The software used was Colour Reader, a free and open-source software downloaded from the Android mobile app market.

2.3. Culture and Preparation of Phages

The phages were purified using the bilayer medium method. First, the already purified bacterial stock solution was diluted to 10^7 CFU/mL, and 100 μL of 10^7 CFU/mL bacteria was added to 1 mL of LB broth until the broth was slightly cloudy. The already purified phage solution was diluted 10-fold to obtain a concentration of 10^2–10^9 PFU/mL of phage solution for further use. The semi-solid (0.7% agar by volume) was heated in the medium using a muffle until it was completely melted, and then it was dispensed into 3 mL centrifuge tubes. In total, 100 μL of diluted bacteria and 100 μL of phage solution of different concentrations were placed in 3 mL centrifuge tubes. The solution was well shaken and poured onto the plate.

The densities of the phage spots in the Petri dishes were dependent on the concentration of phage. The cultured phage Petri dishes were placed in a biosafety cabinet, 3 mL LB bouillon was added, and the medium containing phage, as well as the LB bouillon, was scraped into a 50 mL centrifuge tube using a sterilized glass spatula. The scraped mixture was centrifuged at 8000 rpm for 30 min, and the liquid was then passed through a disposable paper membrane filter with a pore size of 0.22 um. Two purifications were required to obtain the final phage for the experiment. The concentration of phage was determined by the plate counting method.

2.4. Culture and Preparation of Bacteria

In the biological safety cabinet, a small amount of *E. coli*, *S.a*, and *S.T* was scraped from the bacteriophage plate using an alcohol-sterilized catch ring and placed into 3 mL

LB broth, which was sterilized in an autoclave (120 °C, 2 h) and incubated overnight in a shaker (37 °C, 180 rmp) until it gradually became turbid. The concentration of bacteria was calculated using the plate counting method. First, the bacteria were serially diluted 108 times using PBS (the dilution was performed 10 times), and 100 μL of the diluted solution was taken and inoculated in a semi-solid Petri dish and incubated in a 37 °C thermostat for 24 h. The bacterial concentration of the original solution was calculated by counting the plaque numbers on the dish.

2.5. Phage Specificity and Probe Activity

A total of 100 μL 10^{11} PFU/mL of phage stock solution was added to PBS (pH = 7.4, 0.01 M) and diluted stepwise to 10^8 CFU/mL. Then, 100 μL 10^8 PFU/mL of phage was taken; 10 μL SYTO13 (5 mM, 250 μL) was added to the experimental group; 10 μL water was added to the control group; and 100 μL 10^7 CFU/mL *E. coli*, *S.a*, and *S.T* was treated as the phage culture and incubated overnight in Petri dishes in a 37 °C incubator.

A total of 100 μL 10^{11} PFU/mL of phage stock solution was added to PBS (pH = 7.4, 0.01 M) and diluted stepwise to 10^8 CFU/mL. Then, 100 μL 10^8 PFU/mL of phage was taken, and 10 μL SYTO13 (5 mM, 250 μL) was added to the experimental group. Simultaneously, 10 μL water and 100 μL 10^7 CFU/mL *E. coli*, *S.a*, and *S.T* were spiked into the control group and proliferated overnight in a 37 °C incubator. Then, the phage specificity and probe activity were discussed.

2.6. Synthesis of Phage @ DNA Probes

A total of 450 μL 10^{10} PFU/mL phage was mixed with 50 μL 0.1 mg/mL dye in a 1 mL centrifuge tube. Afterwards, it was shaken for 30 s and incubated for 10 min. The tube was then placed into a 50 kd dialysis tube and centrifuged for 5 min at 8000 rpm. The phage's molecular weight (MW) was much larger than 50 kd, and it could not pass through the dialysis membrane. Though the free SYTO dye, with a MW of approximately 320, could pass through the membrane pores, the membrane retained the dye-modified phage, as the free dye had no fluoresce, and the dye bound to the phage emitted green fluorescence under 360 nm excitation light. Therefore, after ultrafiltration, the upper solution of the filter membrane was taken out, and the emitted light at 520 nm was measured using a fluorometer under 365 nm excitation. Then, 50 μM of another phage@SYTO (*E. coli*) was taken and incubated with *S.A*, *S.T*, *V.P*, *E. coli*, and the mixture for 20 min, respectively, and excited by blue light from a fluorescence microscope.

2.7. Detection of Escherichia coli O157:H7 (E. coli) in Fishes

The food samples (shrimp, fish, and others) were mixed with 100 mL 100 μM PBS (pH 7.5) for 10 min. Then, the supernatant was collected for further detection. Firstly, 10 μL of 1 μM pahge@SYTO was mixed with the 100 mL supernatant solution and then agitated (200 rpm on the vortex machine) for 10 min at room temperature. After that, the mixture solution was passed through a micropore membrane filter with a pore size of 450 nm using a syringe. The *E. coli*-phage@SYTO complex (whose size was larger than 1.2 μm) could be separated and retained on the membrane, whereas the free probes, whose size was approximately 200 nm, could pass through the pores. The paper chip was first dried, and then the fluorescent (FL) detection was performed on the paper chip after excitation at 360 nm. All the test samples were placed in a black box, being unaffected by ambient light, and the FL intensity was recorded using a smartphone. Different color intensities can be employed for different concentrations of analytes to determine the presence of some bacterial strains without using any analytical apparatus. We also designed an improved version of the portable fluorimeter by separating the different concentrations into different sections in order to introduce the respective phage@SYTO probes. Images of the spiked samples, as well as the real samples, were taken with an Android smartphone. The distance between the excitation light source and the sample was kept constant (30 cm) during the measurements. For each sample, the data for five points were detected from the

center to the edge of the same sample according to the five-point sampling method. The photographed photos were also imported into the analytical software, which enabled the color fluorescence image of the sample to be divided into red (R), green (G), and blue (B) channels by reading the G value of the paper chip's surface and comparing it to the G_0 read from the paper chip with the uncaptured bacteria. The G/G_0 was employed for the qualification of the targets.

3. Results and Discussion

3.1. Characterization of the Phage@SYTO Probes

SYTO 13 is a specific phage dye which cannot emit fluorescent light by itself, but can emit fluorescence light after the staining of the phage. From Figure 2, it can be seen that 10 µg/mL of phage@SYTO could emit strong fluorescence light after being excited at 365 nm, whereas the dye itself could only emit negligible light and the phage did not emit any light. All these findings illustrated that the phage@SYTO probes had been successfully prepared. From the FL intensity of the phage@SYTO, it can be seen that the SYTO could penetrate the phage's DNA [18].
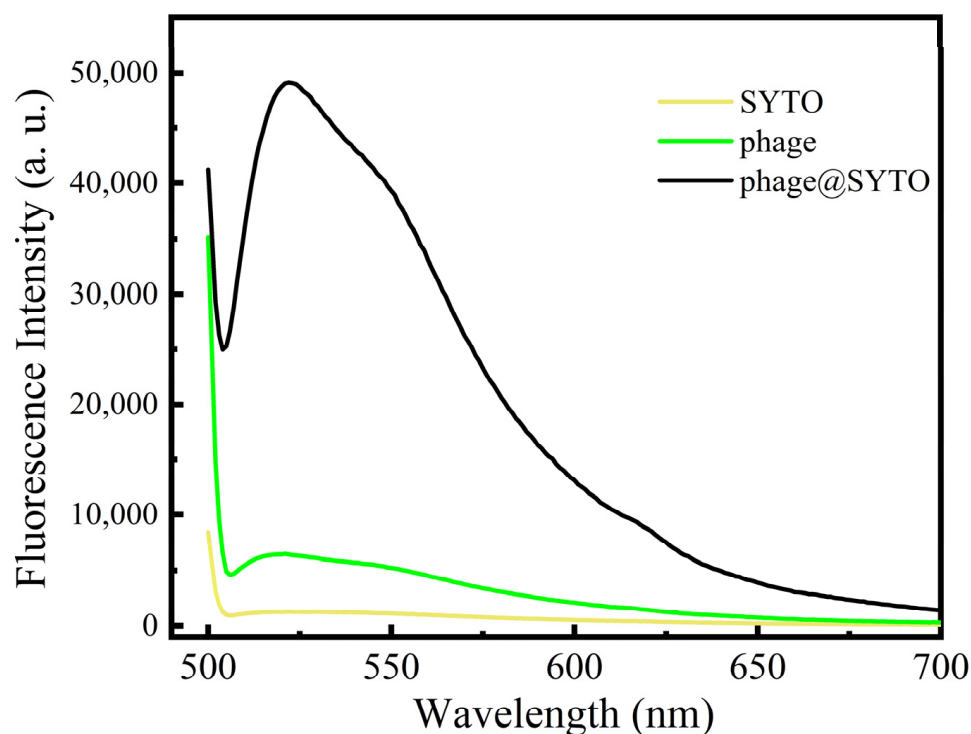

Figure 2. The fluorescent light of 10 µg/mL phage@SYTO probes, SYTO, or phage only.

3.2. The Phage Specificity and Probe Activity

The activity of the probe had a significant effect on the experimental results. Therefore, a comparison of the activity of the phage@SYTO and pure phage was conducted. The comparison shown in Figure 3A,D revealed no significant change in the number of phage spots after the SYTO 13 modification, indicating that the dye had no effect on the activity of the phage. Moreover, the probe was still able to identify the specific bacteria. In addition, as shown in Figure 3A,D, it was found that the plate with spiked *E. coli* produced phage spots. By comparison, Figure 3B,E and Figure 3C,F, which represent the *S.A* and *V.P* plate with the addition of the phage@SYTO probes, depicted no significant plaques. All of these findings indicated that the phage@SYTO was specific to *E. coli*, but not other bacteria.
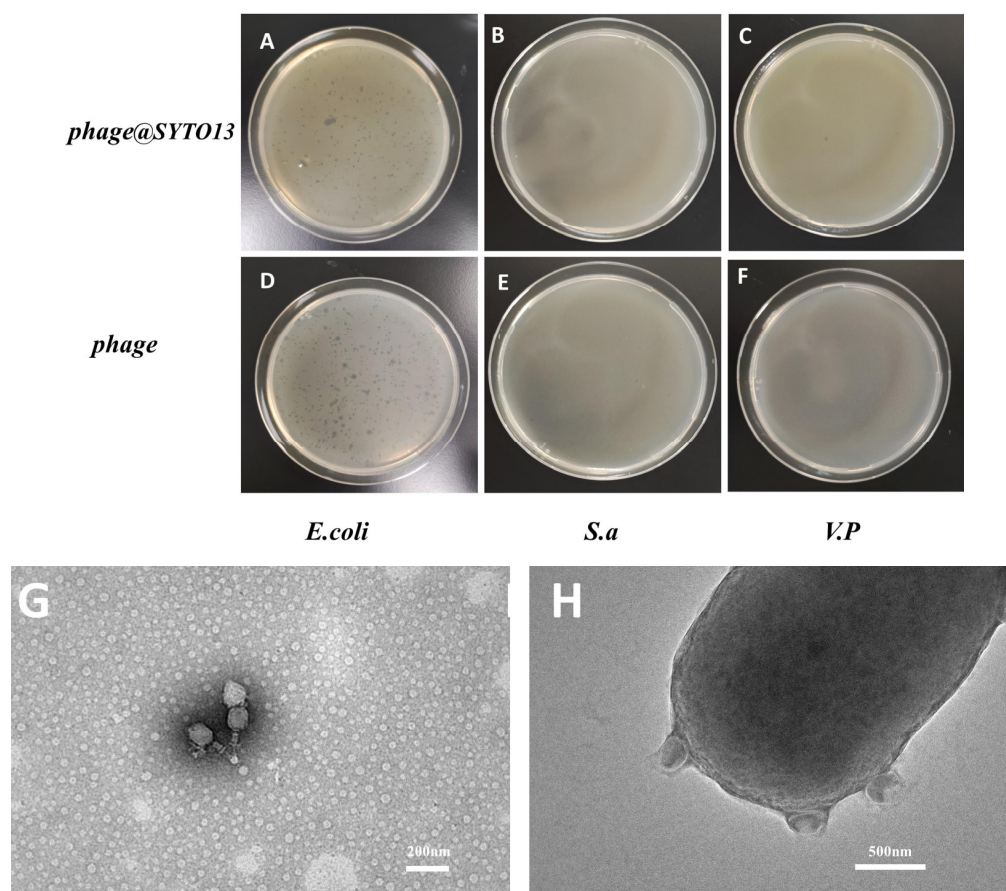
Figure 3. The plaques produced after mixing the 10^5 PFU/mL phage and phage@SYTO on plates containing (**A,D**) *E. coli* O157:H7, (**B,E**) *S.a*, or (**C,F**) *V.P*. The TEM of the (**G**) phage and (**H**) phages surrounding *E. coli* O157:H7.

Furthermore, transmission electron microscopy (TEM) was employed to reveal the formation process of the plaques. As shown in Figure 3G, phages with heads and tails of approximately 200 nm in length could be found. In Figure 3H, there are a large number of phages adhered to the outer cells of *E. coli* O157. The results indicated that the phage has a strong affinity for *E. coli* O157:H7.

3.3. Principle of the Assay

From Figure 4, it can be seen that the phage@SYTO could only bind with *E. coli* to emit fluorescence light. Moreover, the mixture of *E. coli* with other bacteria could also emit fluorescence light. These findings demonstrated that the phage@SYTO has enough specificity and discrimination capacity to identify the target bacteria [19,20]. The labeling of the SYTO amount on the probes was very important for the detection sensitivity. An amount of 100 μL SYTO-13 at different concentrations was mixed with 100 μL 10^9 PFU/mL phage. The changes in fluorescence light intensity (I) were continuously recorded with the change in the dye concentration. Because SYTO-13 only emitted fluorescence light when combined with the phage to form the phage@SYTO, the labeled amount of SYTO-13 on the phage@SYTO could reach saturation after the fluorescence intensity reached its highest level. According to the amount of SYTO-13 material at this time point, the amount of SYTO-13 in each phage could be calculated. According to the highest peak intensity of SYTO-13 at 0.1 μM, we calculated approximately 60,200 SYTO on each phage (equation: 10^{-7} M $\times$ 10^{-4} L $\times$ 6.02×10^{23} / 10^8 PFU = 60,200 SYTO/phage).
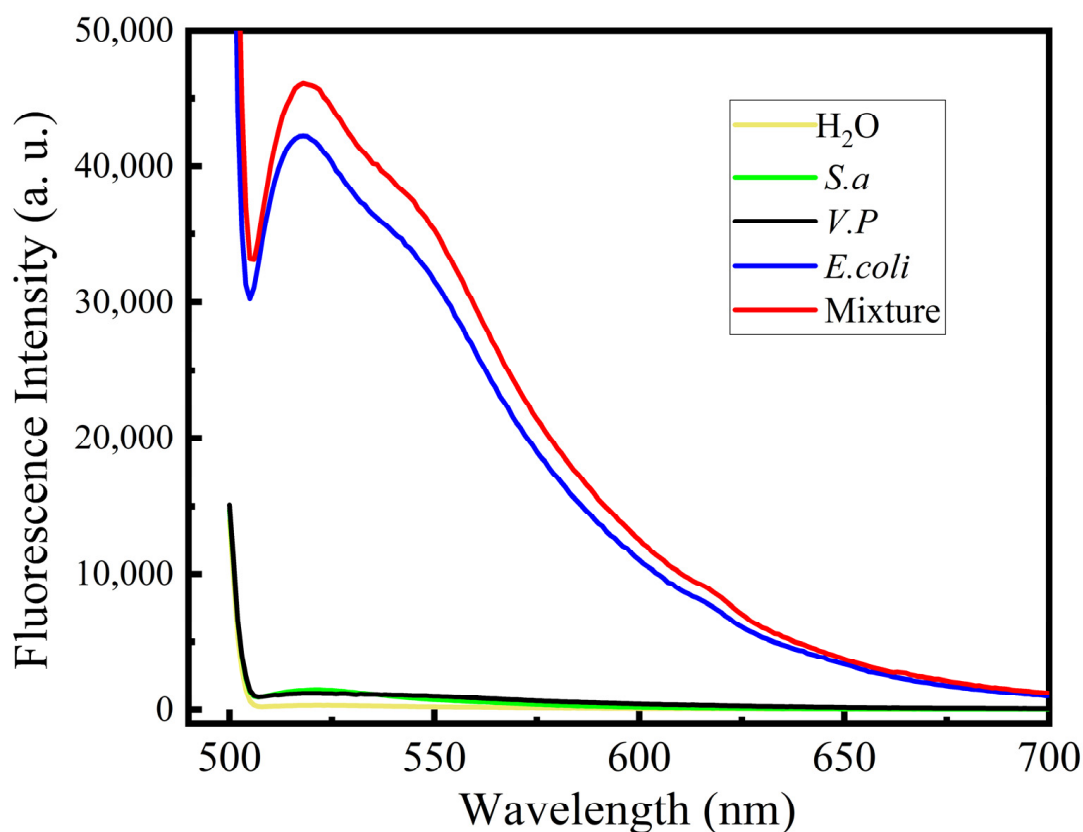
Figure 4. The fluorescence light of the phage@SYTO probe for different targets.

3.4. The Optimization of the Assay

In order to improve the detection performance of this strategy, several reaction conditions were optimized (the concentration of *E. coli* in the optimization experiment was 10^5 CFU/mL). We first optimized the binding time for the phage@SYTO to bind to the pathogenic bacteria *E. coli*. It can be seen from Figure 5A that the optimal binding time was 20 min. The bacteria's surface combined more easily with the phage@SYTO, which meant that the phage did not lose its bioactivity during labeling with SYTO. In the detection process, the concentration of phage@SYTO was also crucial, as a probe concentration that is too low will prevent the phage from fully combining with the target bacteria when the concentration of bacteria is high. However, if the probe concentration is too high, they will be stained on the membrane easily; thus, the background signal will be too high. As can be seen from Figure 5B, the optimum concentration of phage@SYTO was 10^8–10^9 PFU/mL, and the signal to noise ratio (I/I_0) reached its highest value. If the concentration is too high, there will be a strong background signal, even if the signal from *E. coli*-phage@SYTO is high. Taken together, the amount of 10^8 PFU/mL phage@SYTO was selected for the detection. The membrane pore size was also very important for the filtering of the unbound phage@SYTO. From Figure 5C, we can see that the optimum membrane pore size was 0.45 μm, whereas 0.25 μm retained too much phage@SYTO in the solution. Moreover, with a 1 μm pore size, the *E. coli*-phage@SYTO could also pass through the pores, leading to a lower signal. The reaction pH was also optimized, and we found that pH 5.0 to 8.0 was the suitable reaction pH. From Figure 6D, we can see that a pH that was too low or high resulted in a lower FL signal. This may be due to the fact that the phage@SYTO could not combine well with the bacteria. The usual pH of the sample solution was between 5 and 8; therefore, the assay was suitable for many types of real samples.
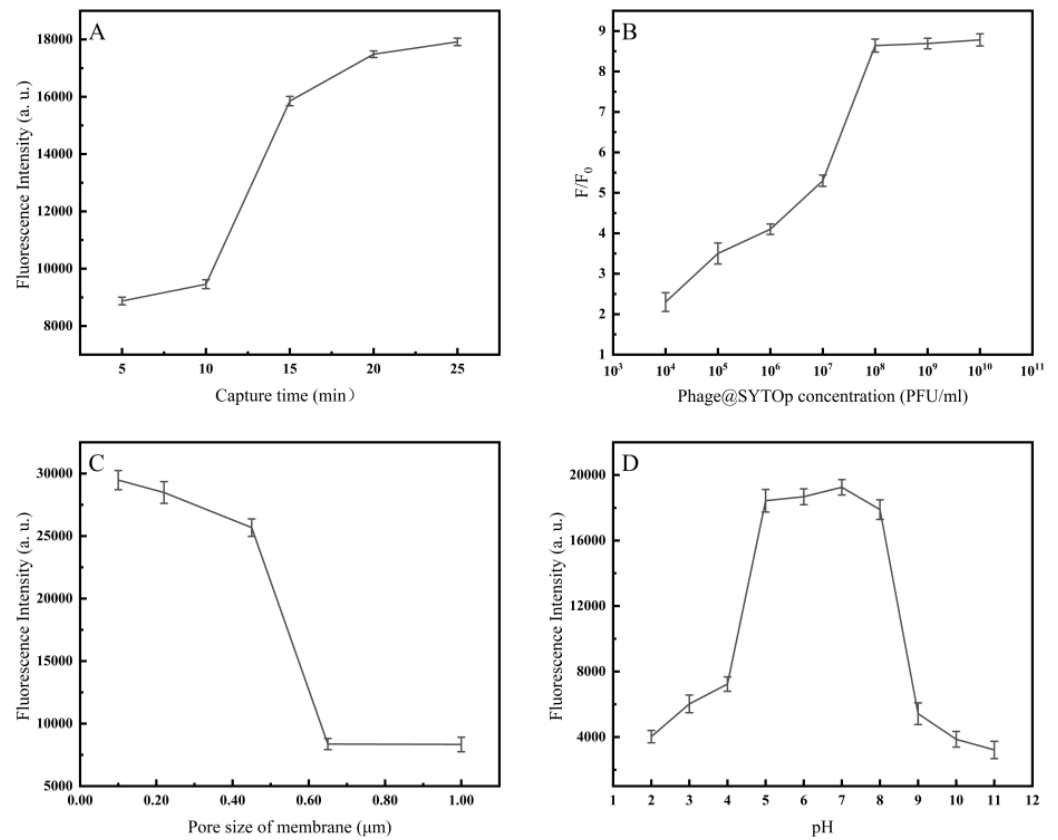
Figure 5. Optimization of experimental conditions: (**A**) phage@SYTO capture time; (**B**) phage@SYTO13 concentration; (**C**) pore size of membrane; (**D**) reaction pH.
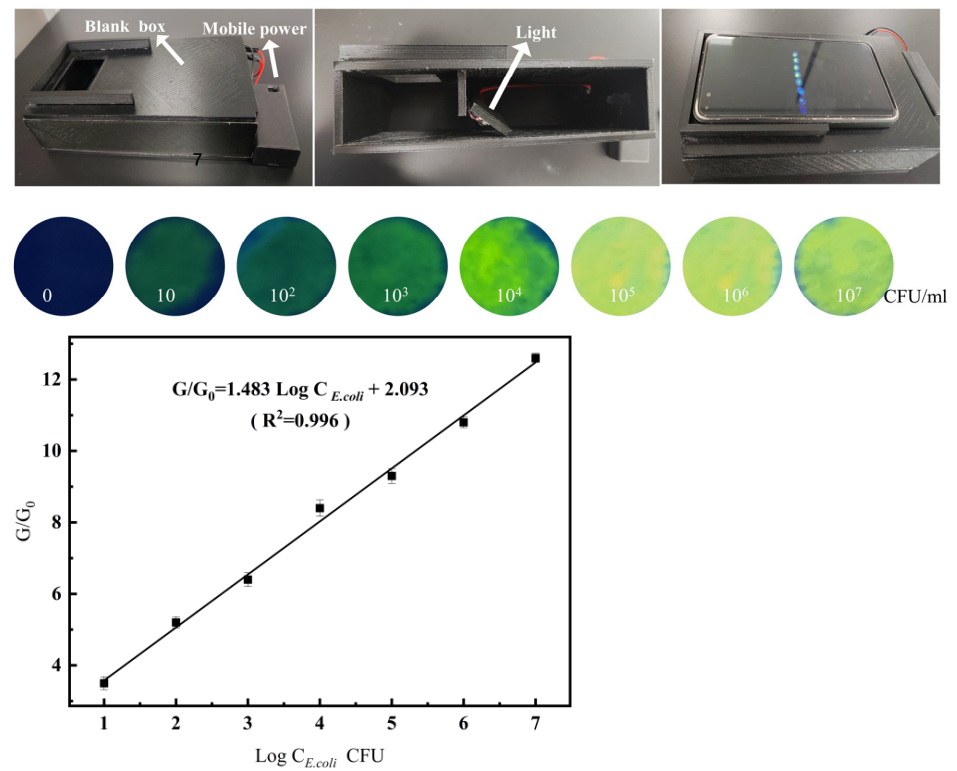

Figure 6. The calibration line of *E. coli* at different concentrations and its FL signals detected by a smartphone.

3.5. Determination of E. coli in the Real Samples

Under the optimal experimental conditions, *E. coli* was diluted with PBS to different concentrations (10^6, 10^5, 10^4, 10^3, 10^2, 10 CFU/mL) for visual fluorescence detection and subsequent microfluidic chip analysis. For visual fluorescence detection, we used different concentration gradients of *E. coli* Figure 6). It can be found that as the concentration of *E. coli* increased, the visualized fluorescence gradually increased. It was easy to observe 10^3 CFU/mL *E. coli* with the naked eye, and no fluorescence could be observed with the naked eye at 100 and 10 CFU/mL. Therefore, the lower limit of detection for visualizing fluorescence with the naked eye was 10^3 CFU/mL.

In addition, this method was compared with some reported *E. coli* detection methods (Table 1). Despite the shortcomings of the drop method, the prepared phage DNA probes still had a better detection range and lower limit of detection compared with the other methods. This is because phages are highly specific to the target bacteria. At the same time, rolling circle amplification (RCA) of the DNA on the phage can amplify the length of the DNA chain by tens of thousands of times, greatly reducing the detection limit.

Table 1. Comparison with *E. coli* detection methods in the literature.

Method	Linear Range (CFU/mL)	LOD (CFU/mL)	Time	Ref.
Nanogap network electrochemical method	10^3–10^8	10^2	>3 h	[28]
SERS	1.0×10^3–5.0×10^7	10^2	~30 min	[29]
The fiberoptic surface plasmon resonance method	1.5×10^3–1.5×10^5	5.0×10^2	45 min	[30]
Field environment monitoring	10^3–10^8	200	40 min	[31]
Fluorescence method	10–10^6	14	2 h	[32]
This work (fluorimeter)	10^3–10^6	300	45 min	[33]
This work	10^2–10^6	50	10 min	

3.6. Specificity, Stability, and Precision of the Sensor

To assess the method's anti-interfering capacity for *E. coli*, we included *Salmonella typhimurium* (*S.T*), *Staphylococcus aureus* (*S.A*), *Listeria monocytogenes* (*L.M*), *Vibrio vulnificus* (*V.V*), and *Vibrio parahaemolyticus* (*V.P*) in the comparison, and the concentration of the other bacteria was 10^7 CFU/mL, except for *E. coli*, which was 10^5 CFU/mL. As shown in Figure 7A, the difference in the signals indicated that other bacteria did not interfere with the detection of *E. coli*. In addition, some common ions in the sample solution were selected to perform anti-interference experiments. As shown in Figure 7B, the effects of the above substances on the detection of *E. coli* were negligible. The above results show that the phage sensor has a good specificity and anti-interference ability for the detection of the target bacteria. The assay was used to detect 10^6 CFU/mL of *E. coli* five times using the same batch of phage@SYTO probes. The RSD was lower than 7%, which proved that the sensor showed high stability. We also tested the same sample over 5 days of storage using the same batch of phage@SYTO probes, and the RSD was 5.8%. This indicated that the probe showed approximately 5 days of stability. Moreover, the inter- and intra-precision were detected using 10^6 CFU/mL of *E. coli*. The *RSD* values were 5.3% and 6.2%, respectively. All of these findings demonstrated that the sensor exhibited high precision.

To evaluate the potential application of this strategy, some samples mixed with different concentrations of *E. coli* were tested. The results are summarized in Table 2. The recovery rates of *E. coli* in the pork samples ranged from 95.2% to 102%. Compared with the ELISA method for the rapid detection of *E. coli*, the detection limit of this method is lower,

which further illustrates the superiority of this method. The above conclusion demonstrates that the proposed sensing platform can be used for *E. coli* in food samples.
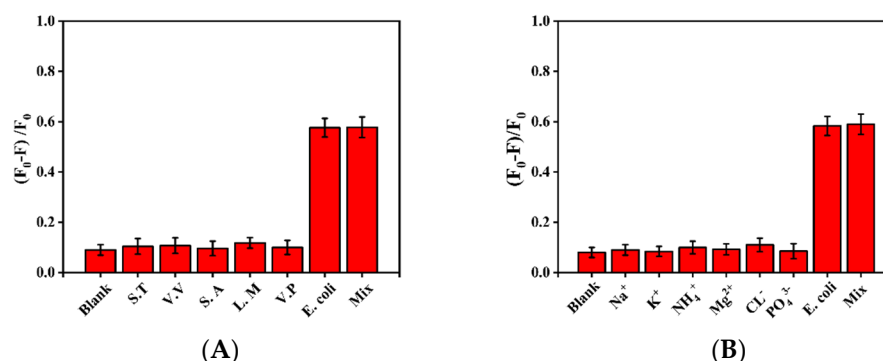

Figure 7. (**A**) The bacterial specificity based on paper chip analysis. (**B**) The resistance ability formicrofluidic chip bacteria analysis based on matrix interference.

Table 2. Detection of *E. coli* in real samples using the proposed method (*n* = 5).

Samples	Spiked (CFU/mL)	Measured (CFU/mL)	Recovery (%)	RSD (%)	ELISA (CFU/mL)
Fish 1	0	ND			ND
	10^3	$(0.95 \pm 0.06) \times 10^3$	95.2	6.5	ND
	10^5	$(0.98 \pm 0.05) \times 10^5$	98.1	5.4	$(1.18 \pm 0.10) \times 10^5$
Fish 2	0	ND			ND
	10^3	$(0.96 \pm 0.05) \times 10^3$	96.3	5.9	ND
	10^5	$(1.02 \pm 0.07) \times 10^5$	102	6.8	$(0.94 \pm 0.19) \times 10^5$
Shrimp 1	0	ND			ND
	10^3	$(1.01 \pm 0.05) \times 10^3$	101	4.7	ND
	10^5	$(0.99 \pm 0.06) \times 10^5$	99.4	6.1	$(1.10 \pm 0.14) \times 10^5$

ND: No detection.

4. Conclusions

In conclusion, the fabricated FL phage sensor can be used to POC quantify *E. coli* O157 bacteria in foods. Its particular merits illustrate the simplicity of its manipulation. It avoids the need for the employment of any precise instrumentation or trained persons. It also has sufficient sensitivity, a wide detection range, and high selectivity. The LOD for the bacteria is below 100 CFU/mL, which meets the standards established by governmental agencies for *E. coli* O157. Although it is comparable to ELISA, the new paper-chip-based platform has the potential to be developed as a simple, portable, sensitive, and low-cost analytical tool for immediate bacterial diagnosis and POC tests of food safety.

Author Contributions: Conceptualization, writing—original draft, investigation, validation, writing—review and editing, C.W.; methodology, conceptualization, supervision, writing, funding acquisition, N.G.; conceptualization, writing—review and editing, D.L.; writing—review and editing, Q.J. All authors have read and agreed to the published version of the manuscript.

Institutional Review Board Statement: Not applicable.

Informed Consent Statement: Not applicable.

Data Availability Statement: Not applicable.

Conflicts of Interest: The authors declare no conflict of interest.

References

1. Shi, C.; Qing, X.; Yue, G.; Ling, J.; He, H. Luciferase-Zinc-Finger System for the Rapid Detection of Pathogenic Bacteria. *J. Agric. Food Chem.* **2017**, *65*, 6674–6681. [CrossRef] [PubMed]

2. Oyedeji, A.B.; Ezekiel, G.; Janet, A.A.; Opeolu, M.O.; Sefater, G.; Martins, A.A.; Samson, A.O.; Oluwafemi, A.A. Metabolomic Approaches for the Determination of Metabolites from Pathogenic Microorganisms: A Review. *Food Res. Int.* **2020**, *140*, 110042. [CrossRef] [PubMed]

3. Martinović, T.; Uroš, A.; Martina, Š.G.; Dina, R.; Djuro, J. Foodborne Pathogens and Their Toxins. *J. Proteom.* **2016**, *147*, 226–235. [CrossRef] [PubMed]

4. Rajapaksha, P.; Elbourne, A.; Gangadoo, S.; Brown, R.; Cozzolino, D.; Chapman, J. A Review of Methods for the Detection of Pathogenic Microorganisms. *Analyst* **2018**, *144*, 396–411. [CrossRef] [PubMed]

5. Carrillo, J.D.; Mayorquin, J.S.; Stajich, J.E.; Eskalen, A. Probe-Based Multiplex Real-Time PCR as a Diagnostic Tool to Distinguish Distinct Fungal Symbionts Associated with *Euwallacea kuroshio* and *Euwallacea whitfordiodendrus* in California. *Plant Dis.* **2019**, *104*, 227–238. [CrossRef] [PubMed]

6. Lv, X.; Huang, Y.; Liu, D.; Liu, C.; Shan, S.; Li, G.; Duan, M.; Lai, W. Multicolor and Ultrasensitive Enzyme-Linked Immunosorbent Assay Based on the Fluorescence Hybrid Chain Reaction for Simultaneous Detection of Pathogens. *J. Agric. Food Chem.* **2019**, *67*, 9390–9398. [CrossRef]

7. Richter, M.F.; Drown, B.S.; Riley, A.P.; Garcia, A.; Shirai, T.; Svec, R.L.; Hergenrother, P.J. Predictive compound accumulation rules yield a broad-spectrum antibiotic. *Nature* **2017**, *545*, 299–304. [CrossRef]

8. Zhang, Y.; Wu, Y.; Wu, Y.; Chang, Y.; Liu, M. CRISPR-Cas systems: From gene scissors to programmable biosensors. *Trends Anal. Chem.* **2021**, *137*, 116210. [CrossRef]

9. Shi, R.; Zou, W.; Zhao, Z.; Wang, G.; Guo, M.; Ai, S.; Zhou, Q.; Zhao, F.; Yang, Z. Development of a sensitive phage-mimotope and horseradish peroxidase based electrochemical immunosensor for detection of O,O-dimethyl organophosphorus pesticides. *Biosens. Bioelectron.* **2022**, *218*, 114748. [CrossRef]

10. Jiang, H.; Yang, J.; Wan, K.; Jiang, D.; Jin, C. Miniaturized Paper-Supported 3D Cell-Based Electrochemical Sensor for Bacterial Lipopolysaccharide Detection. *ACS Sens.* **2020**, *5*, 1325–1335. [CrossRef]

11. Baoqing, Z.; Qinghua, Y.; Fan, L.; Xinran, X.; Yuting, S.; Chufang, W.; Yanna, S.; Liang, X.; Jumei, Z.; Juan, W.; et al. CRISPR/Cas12a based fluorescence-enhanced lateral flow biosensor for detection of *Staphylococcus aureus*. *Sens. Actuators B Chem.* **2021**, *351*, 130906.

12. Bu, S.; Wang, K.; Wang, C.; Li, Z.; Hao, Z.; Liu, W.; Wan, J. Immunoassay for foodborne pathogenic bacteria using magnetic composites Ab@Fe$_3$O$_4$, signal composites Ap@PtNp, and thermometer readings. *Microchim. Acta* **2020**, *187*, 679. [CrossRef]

13. Dieckhaus, L.; Park, T.S.; Yoon, J.-Y. Smartphone-Based Paper Microfluidic Immunoassay of *Salmonella* and *E. coli*. *Methods Mol. Biol.* **2020**, *2182*, 83–101.

14. Liu, S.; Lu, S.; Sun, S.; Hai, J.; Meng, G.; Wang, B. NIR II Light-Response Au Nanoframes: Amplification of a Pressure- and Temperature-Sensing Strategy for Portable Detection and Photothermal Therapy of Cancer Cells. *Anal. Chem.* **2021**, *93*, 14307–14316. [CrossRef]

15. Lee, W.-I.; Park, Y.; Shrivastava, S.; Jung, T.; Meeseepong, M.; Lee, J.; Jeon, B.; Yang, S.; Lee, N.-E. A fully integrated bacterial pathogen detection system based on count-on-a-cartridge platform for rapid, ultrasensitive, highly accurate and culture-free assay. *Biosens. Bioelectron.* **2020**, *152*, 112007. [CrossRef] [PubMed]

16. Laliwala, A.; Svechkarev, D.; Sadykov, M.R.; Endres, J.; Bayles, K.W.; Mohs, A.M. Simpler Procedure and Improved Performance for Pathogenic Bacteria Analysis with a Paper-Based Ratiometric Fluorescent Sensor Array. *Anal. Chem.* **2022**, *94*, 2615–2624. [CrossRef] [PubMed]

17. Shin, J.H.; Hong, J.; Go, H.; Park, J.; Kong, M.; Ryu, S.; Kim, K.-P.; Roh, E.; Park, J.-K. Multiplexed Detection of Foodborne Pathogens from Contaminated Lettuces Using a Handheld Multistep Lateral Flow Assay Device. *J. Agric. Food Chem.* **2017**, *66*, 290–297. [CrossRef] [PubMed]

18. Luo, K.; Kim, H.-Y.; Oh, M.-H.; Kim, Y.-R. Paper-based lateral flow strip assay for the detection of foodborne pathogens: Principles, applications, technological challenges and opportunities. *Crit. Rev. Food Sci. Nutr.* **2018**, *60*, 157–170. [CrossRef] [PubMed]

19. Li, W.; Coulon, F.; Singer, A.; Zhu, Y.-G.; Yang, Z. Paper-Based Devices as a New Tool for Rapid and on-Site Monitoring of "Superbugs". *Environ. Sci. Technol.* **2021**, *55*, 12133–12135. [CrossRef]

20. Yizhong, S.; Yunlong, W.; Chunlei, Z.; Jinxuan, C.; De-Man, H. Ratiometric fluorescent signals-driven smartphone-based portable sensors for onsite visual detection of food contaminants. *Coord. Chem. Rev.* **2022**, *458*, 214442.

21. Lin, B.; Guan, Z.; Song, Y.; Song, E.; Lu, Z.; Liu, D.; An, Y.; Zhu, Z.; Zhou, L.; Yang, C. Lateral flow assay with pressure meter readout for rapid point-of-care detection of disease-associated protein. *Lab A Chip* **2018**, *18*, 965–970. [CrossRef] [PubMed]

22.	Ji, T.; Liu, D.; Liu, F.; Li, J.; Ruan, Q.; Song, Y.; Tian, T.; Zhu, Z.; Zhou, L.; Lin, H.; et al. A pressure-based bioassay for the rapid, portable and quantitative detection of C-reactive protein. *Chem. Commun.* **2016**, *52*, 8452–8454. [CrossRef]

23.	Wei, X.; Tian, T.; Jia, S.; Zhu, Z.; Ma, Y.; Sun, J.; Lin, Z.; Yang, C.J. Microfluidic Distance Readout Sweet Hydrogel Integrated Paper-Based Analytical Device (μDiSH-PAD) for Visual Quantitative Point-of-Care Testing. *Anal. Chem.* **2016**, *88*, 2345–2352. [CrossRef] [PubMed]

24.	Torres-Barceló, C. The disparate effects of bacteriophages on antibiotic-resistant bacteria. *Emerg. Microbes Infect.* **2018**, *7*, 168. [CrossRef]

25.	Sha, L.; Xuliang, H.; Tao, Z.; Kaixuan, Z.; Changhu, X.; Zengrui, T.; Lian, J.; Nongyue, H.; Yan, D.; Song, L.; et al. Highly sensitive smartphone-based detection of Listeria monocytogenes using SYTO9. *Chin. Chem. Lett.* **2021**, *33*, 1933–1935.

26.	You, S.-M.; Jeong, K.-B.; Luo, K.; Park, J.-S.; Park, J.-W.; Kim, Y.-R. Paper-based colorimetric detection of pathogenic bacteria in food through magnetic separation and enzyme-mediated signal amplification on paper disc. *Anal. Chim. Acta* **2021**, *1151*, 338252. [CrossRef] [PubMed]

27.	Yuwei, R.; Lulu, C.; Xiyan, Z.; Rui, J.; Dexin, O.; Yang, W.; Danfeng, Z.; Yizhong, S.; Na, L.; Yingwang, Y. A novel fluorescence resonance energy transfer (FRET)-based paper sensor with smartphone for quantitative detection of Vibrio parahaemolyticus. *Food Control* **2022**, *145*, 109412.

28.	Lei, J.; Shi, L.; Li, B.; Yang, C.J.; Jin, Y. Ultrasensitive and portable assay of mercury (II) ions via gas pressure as readout. *Biosens. Bioelectron.* **2018**, *122*, 32–36. [CrossRef]

29.	Niazi, M.; Alizadeh, E.; Zarebkohan, A.; Seidi, K.; Ayoubi-Joshaghani, M.H.; Azizi, M.; Dadashi, H.; Mahmudi, H.; Javaheri, T.; Jaymand, M.; et al. Advanced Bioresponsive Multitasking Hydrogels in the New Era of Biomedicine. *Adv. Funct. Mater.* **2021**, *31*, 2104123. [CrossRef]

30.	Jung, I.Y.; Kim, J.S.; Choi, B.R.; Lee, K.; Lee, H. Hydrogel Based Biosensors for In Vitro Diagnostics of Biochemicals, Proteins, and Genes. *Adv. Healthc. Mater.* **2017**, *6*, 1601475. [CrossRef]

31.	Pinelli, F.; Magagnin, L.; Rossi, F. Progress in hydrogels for sensing applications: A review. *Mater. Today Chem.* **2020**, *17*, 100317. [CrossRef]

32.	Liang, Y.; He, J.; Guo, B. Functional Hydrogels as Wound Dressing to Enhance Wound Healing. *ACS Nano* **2021**, *15*, 12687–12722. [CrossRef] [PubMed]

33.	He, X.; Yang, Y.; Guo, Y.; Lu, S.; Du, Y.; Li, J.-J.; Zhang, X.; Leung, N.L.C.; Zhao, Z.; Niu, G.; et al. Phage-Guided Targeting, Discriminated Imaging and Synergistic Killing of Bacteria by AIE Bioconjugates. *J. Am. Chem. Soc.* **2020**, *142*, 3959–3969. [CrossRef] [PubMed]